Semiconductors, 2022, Vol. 56, No. 5

Temperature dependence of the Fermi level in HgCdTe narrow-gap bulk films at different mercury vacancy concentrations

© D.V. Kozlov[1,2], M.S. Zholudev[1,2], V.V. Rumyantsev[1,2], A.V. Ikonnikov[3],
S. Pavlov[4], H.-W. Hübers[4,5], S.V. Morozov[1,2]

[1] Institute of Physics of Microstructures, Russian Academy of Sciences,
603950 Nizhny Novgorod, Russia
[2] Lobachevsky State University of Nizhny Novgorod,
603022 Nizhny Novgorod, Russia
[3] Lomonosov Moscow State University (Department of Physics),
119991 Moscow, Russia
[4] Institute of Optical Sensor Systems German Aerospace Center (DLR),
12489 Berlin, Germany
[5] Institut für Physik, Humboldt-Universität zu Berlin,
12489 Berlin, Germany

E-mail: dvkoz@ipmras.ru

Received December 25, 2021
Revised December 30, 2021
Accepted December 30, 2021

We calculate Fermi level position in bulk HgCdTe with cadmium fraction from 19 to 22% as a function of temperature for different concentrations of mercury vacancies forming double-charged acceptors with ionization energies of 11 and 21 meV for neutral and singly charged states respectively. The concentration of free carriers in the bands at different temperatures and the proportion of acceptor centres in different charge states are calculated as well. The results explain the fast temperature quenching of photoconductivity involving the vacancies states. It is also shown that in a *p*-type material conductivity dependence on temperature includes an exponential growth region with a characteristic energy much greater than a half of the bandgap at zero temperature expected for an intrinsic semiconductor.

Keywords: narrow-gap semiconductors, HgCdTe, Fermi level, doubly charged acceptors.

DOI: 10.21883/SC.2022.05.53424.9789

1. Introduction

Solid-state solutions of $Hg_{1-x}Cd_xTe$ (CHT) have been studied for over four decades, which is due to their leading position as a material for photodetectors [1,2]. It is well known that bulk HgTe is a zero-gap semiconductor with a so-called negative band gap, while CdTe is a relatively high band gap (band gap $E_g \sim 1.6\,\text{eV}$) semiconductor. This potentially makes it possible to implement photodetector and light-emitting devices based on ternary solutions or heterostructures with quantum wells (QWs) in a wide range of the spectrum: from near infrared (IR) wavelength range to far IR (terahertz (THz)) wavelength range [3]. The practical need for photodetectors of the near and medium IR range, including photo-integrated matrices, determined the corresponding development of the technology of epitaxial growth of layers of ternary HgCdTe solutions and the formation of device structures based on them. More towards, this applies to relatively wide-band layers, on the basis of which photodetectors for wavelength ranges of $1-3$, $3-5$, $8-10\,\mu$m [4] are currently being produced. The study of more narrow-bandgap layers, as well as heterostructures with CHT-based QWs, was long held back by the limited growth possibilities of such structures, and only relatively recently significant progress has been made in the technology of molecular-beam epitaxy (MBE) of structures based on HgCdTe, which revived interest in studying their properties [5,6]. At the same time, the focus in the studies of such structures shifted to the area of effects caused by the law of dispersion of charge carriers and inversion of bands, in particular, the occurrence of the state of a topological insulator in two-dimensional [7] and three-dimensional structures [8] were shown, the presence of pseudo-relativistic particles — massless Dirac fermions in massless QWs [9] and Kane fermions in volume CHT films [10–12]. CHT-based structures may prove to be a promising material for the creation of detectors and radiation sources in the far and medium infrared range, in particular, for designing of interband lasers [13,14] and for applications in the field of absorption and heterodyne spectroscopy with time resolution in long-wavelength part of the medium IR range (radiation wavelength is $9-30\,\mu$m).

One of the main issues in the development of optoelectronic applications based on HgCdTe in the indicated directions is strong dependence of the carrier lifetime on the concentration of impurity-defect centers due to recombination by the Shockley–Reed–Hall (SRH) mechanism [15]. The most common CHT defect, which is inevitably present in the material due to the weakness of the mercury–

tellurium chemical bond, is a mercury vacancy. The mercury vacancy is a divalent or double acceptor, which can be in three charge states: 1) neutral A_2^0-center (two holes are connected to acceptor); 2) partially-ionized A_2^{-1}-center (one hole is connected to acceptor); 3) fully-ionized A_2^{-2}-center, free of holes.

Mercury vacancies are mentioned in many papers (see, for example, [16–20]), but currently there is no consensus on the spectrum of hole states for such acceptors, including ionization energies A_2^0-center and A_2^{-1}-center, as also is no detailed theory that accurately describes the spectrum of states of „two-charge“ centers. The analysis of absorption spectra in semiconductors with two-charge centers is of considerable complexity due to the need to find partial concentrations of charge carriers at different states of such centers, which is a complex problem requiring additional experimental data and their analysis, as, for example, for double donors in silicon [21], where the bond energy of the centers much smaller than the band gap and the problem is unipolar. If it is necessary to take into account carrier concentrations in both zones, as for narrow-bandgap CHT, the complexity of such calculations increases. This complicates the analysis of the observed photoconductivity (PC) and photoluminescence (PL) spectra, as well as the interpretation of the measured carrier lifetimes, which requires detailed data on the concentration of acceptors and the degree of their compensation. It is necessary to understand how mercury vacancies are distributed by charge states, and how carriers are distributed by energy levels of such charge states. In recent studies, the ionization energies of neutral and singly ionized mercury vacancies for narrow-bandgap HgCdTe films (11 and 21 meV, respectively) grown on the GaAs substrate by molecular-beam epitaxy [22–24] were experimentally obtained from the analysis of the spectra of PC and PL. For A_2^0-center this energy was 11 ± 2 meV, for A_2^{-1}-center — 21 ± 2 meV.

In this work, the temperature dependence of the position of the Fermi level in volume HgCdTe with different concentrations of residual shallow donors and doubly charged acceptors (mercury vacancies) is analyzed. The concentration of free carriers in the bands at different temperatures and the fraction of acceptor centers in different charge states were also calculated. The results obtained explain the rapid temperature quenching of the PC associated with doubly charged acceptors and show that in a p-type material, depending on the electron concentration on temperature, the „activation“ region with the energy much higher than $0.5E_g(T = 0)$ can be observed, as might be expected from the law of mass action for the intrinsic semiconductor.

2. Calculation method

To calculate the concentration of equilibrium carriers in the bands and „impurity“ states, the electroneutrality equation was solved:

$$n + N_A^{-1} + 2N_A^{-2} = p + N_D^{+1}, \tag{1}$$

where n is concentration of electrons in the conduction band, p is concentration of holes in the valence band, N_A^{-1} is concentration of doubly charged acceptors with one captured electron (state A_2^{-1}), N_A^{-2} is concentration of doubly charged acceptors with two captured electrons (state A_2^{-2}), N_D^{+1} is concentration of ionized donors.

It was assumed that there are not enough free carriers to form the degenerated Fermi-gas, so the dependence of their concentration on temperature T is calculated by the formulas:

$$n = N_c(T)\exp\left(\frac{\mathrm{F} - E_c}{T}\right), \tag{2}$$

$$p = N_v(T)\exp\left(\frac{E_v - \mathrm{F}}{T}\right), \tag{3}$$

where F is Fermi energy, E_c is energy of the bottom of the conduction band, E_v is energy of the top of the valence band, and N_c and N_v are effective densities of states in the conduction band and in the valence band, respectively. On the energy scales under consideration, we can assume that the dispersion law in these zones is parabolic with high accuracy; therefore, these quantities are calculated by the formula

$$N_{c,v} = \frac{2}{\hbar^3}\left(\frac{m_{c,v}T}{2\pi}\right)^{3/2}, \tag{4}$$

where m_c and m_v are effective masses in the conduction band and valence band, respectively.

The concentration of ionized donors is

$$N_D^{+1} = \frac{N_D}{1 + g_D\exp(\frac{\mathrm{F}-E_D}{T})}, \tag{5}$$

where N_D is overall concentration of donors, $E_D = 1$ meV is energy of the donor's ground state (estimated within the framework of a hydrogen-like model), and $g_D = 2$ is degeneracy multiplicity of the donor's ground state.

The concentrations of singly and doubly charged acceptors are, respectively,

$$N_A^{-1} = N_A\frac{g_1(T)}{A(T)}\exp\left(\frac{\mathrm{F} - E_A^{(1)}}{T}\right), \tag{6}$$

$$N_A^{-2} = N_A\frac{g_2(T)}{A(T)}\exp\left(\frac{2\mathrm{F} - E_A^{(1)} - E_A^{(2)}}{T}\right), \tag{7}$$

where N_A is the total concentration of doubly charged acceptors, $E_A^{(1)}$ is the energy required to capture electron from the valence band by neutral acceptor, $E_A^{(2)}$ is the energy required to capture electron from the valence band by the singly charged acceptor; the normalization factor is equal to

$$A(T) = 1 + g_1(T)\exp\left(\frac{\mathrm{F} - E_A^{(1)}}{T}\right) + g_2(T)\exp\left(\frac{2\mathrm{F} - E_A^{(1)} - E_A^{(2)}}{T}\right), \tag{8}$$

and the effective densities of states are equal to

$$g_1(T) = g_1^{(0)} + \sum_{n=1,2,\ldots} g_1^{(n)} \exp\left(\frac{E_A^{(1)} - E_{A,n}^{(1)}}{T}\right), \tag{9}$$

$$g_2(T)=g_2^{(0)}+\sum_{n=1,2,\ldots} g_2^{(n)} \exp\left(\frac{E_A^{(2)}+E_A^{(1)}-E_{A,n}^{(2)}}{T}\right), \tag{10}$$

where $g_{1,2}^{(0)}$ is the degeneracy multiplicities of the ground one- and two-particle state of the acceptor, and $g_{1,2}^{(n)}$ and $E_{A,n}^{(1,2)}$ are the degeneracy multiplicities and the energies of the excited one- and two-particle states of the acceptor, respectively. Please note that, since the influence of impurity-defect centers on each other is neglected, the sum in the above formula should be cut off as soon as the localization scale of the acceptor state wave function becomes comparable with the average distance between impurity-defect centers. This distance is determined by the concentration of acceptors in the studied CHT films, the typical value is 50–200 nm. The degree of degeneracy of the ground state of the singly ionized acceptor center was assumed to be $g_1^{(1)} = 4$, of the neutral one — $g_2^{(1)} = 6$.

Thus, the electroneutrality equation can be written as follows:

$$N_c \exp\left(\frac{\mathrm{F} - E_c}{T}\right) + \frac{N_A\left(2 + g_1(T)\exp\left(\frac{E_A^{(1)}-\mathrm{F}}{T}\right)\right)}{\left(1 + g_1(T)\exp\left(\frac{E_A^{(1)}-\mathrm{F}}{T}\right) + g_2(T)\exp\left(\frac{E_A^{(2)}-\mathrm{F}}{T}\right)\right)} = N_v \exp\left(\frac{E_v - \mathrm{F}}{T}\right) + \frac{N_D}{\left(1 + 2\exp\left(\frac{\mathrm{F}-E_D}{T}\right)\right)}. \tag{11}$$

As a result of solving these equations, the position of the Fermi level as well as the concentration of free holes in the valence band and the concentrations of singly ionized and neutral acceptor centers, as function of the temperature of CHT were found:

$$N_{A^{-1}} = \frac{N_A g_1(T)\exp\left(\frac{E_A^{(1)}-\mathrm{F}}{T}\right)}{\left(1 + g_1(T)\exp\left(\frac{E_A^{(1)}-\mathrm{F}}{T}\right) + g_2(T)\exp\left(\frac{E_A^{(2)}-\mathrm{F}}{T}\right)\right)}, \tag{12}$$

$$N_{A^0} = \frac{N_A g_2(T)\exp\left(\frac{E_A^{(2)}-\mathrm{F}}{T}\right)}{\left(1 + g_1(T)\exp\left(\frac{E_A^{(1)}-\mathrm{F}}{T}\right) + g_2(T)\exp\left(\frac{E_A^{(2)}-\mathrm{F}}{T}\right)\right)}. \tag{13}$$

3. Results and discussion

Figure 1 shows the temperature-dependence of the concentration of free holes in the valence band of a solid-state solution of CHT, calculated at different values of the band gap of the material (solid lines) at the concentration of acceptors $N_A = 4 \cdot 10^{14}\,\mathrm{cm}^{-3}$ and donors $N_D = 2 \cdot 10^{14}\,\mathrm{cm}^{-3}$. The latter value is the donor concentration estimate in real structures based on the possibility of changing the type of conduction of structures by means of various annealings [25]. The dashed line represents the concentration of holes transferred from divalent acceptors — mercury vacancies. This concentration (p_A) can be calculated as

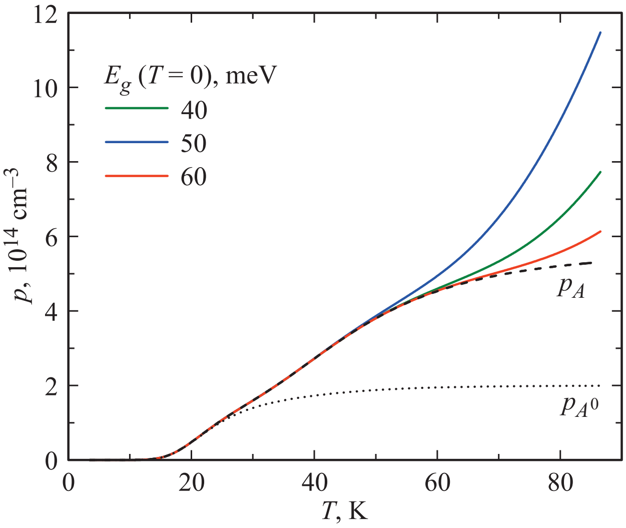

Figure 1. Calculated dependences of the concentration of free holes in $\mathrm{Hg}_{1-x}\mathrm{Cd}_x\mathrm{Te}$ films with different values of the band gap (solid lines) at the concentration of mercury vacancies $4 \cdot 10^{14}\,\mathrm{cm}^{-3}$ and concentrations of shallow compensating donors $2 \cdot 10^{14}\,\mathrm{cm}^{-3}$ (the ionization energy of the donor was assumed equal to 1 meV). Dashed line shows the concentration of carriers transferred from mercury vacancies to the valence band p_A. Dotted line shows the concentration of holes thermally ionized from the states of neutral mercury vacancies into the valence band p_{A^0}.

$$p_A = (2N_A - N_D) - (2N_{A^0} + N_{A^{-1}}). \tag{14}$$

It should be noted that $2N_A - N_D$ is the number of holes in acceptor levels at zero temperature, $2N_{A^0} + N_{A^{-1}}$ is the number of holes associated with acceptor centers at arbitrary temperature. The calculation showed that the number of carriers transferred to the valence band from acceptor centers does not depend on the composition of the solid-state solution.

It can be seen from Fig. 1 that at $T < 15$ K the number of free carriers is negligibly small, while at temperatures above 15 K the number of free holes in the valence band increases rapidly. This explains the effect of „quenching“ of photoconductivity (PC) lines of volume CHT films with increase in temperature, observed in the work [23]: with increase in temperature, the significant dark current appears, and relatively weak photoelectric current signal becomes poorly distinguishable against its background.

In the structure under consideration at low temperature, the concentration of neutral mercury vacancies is

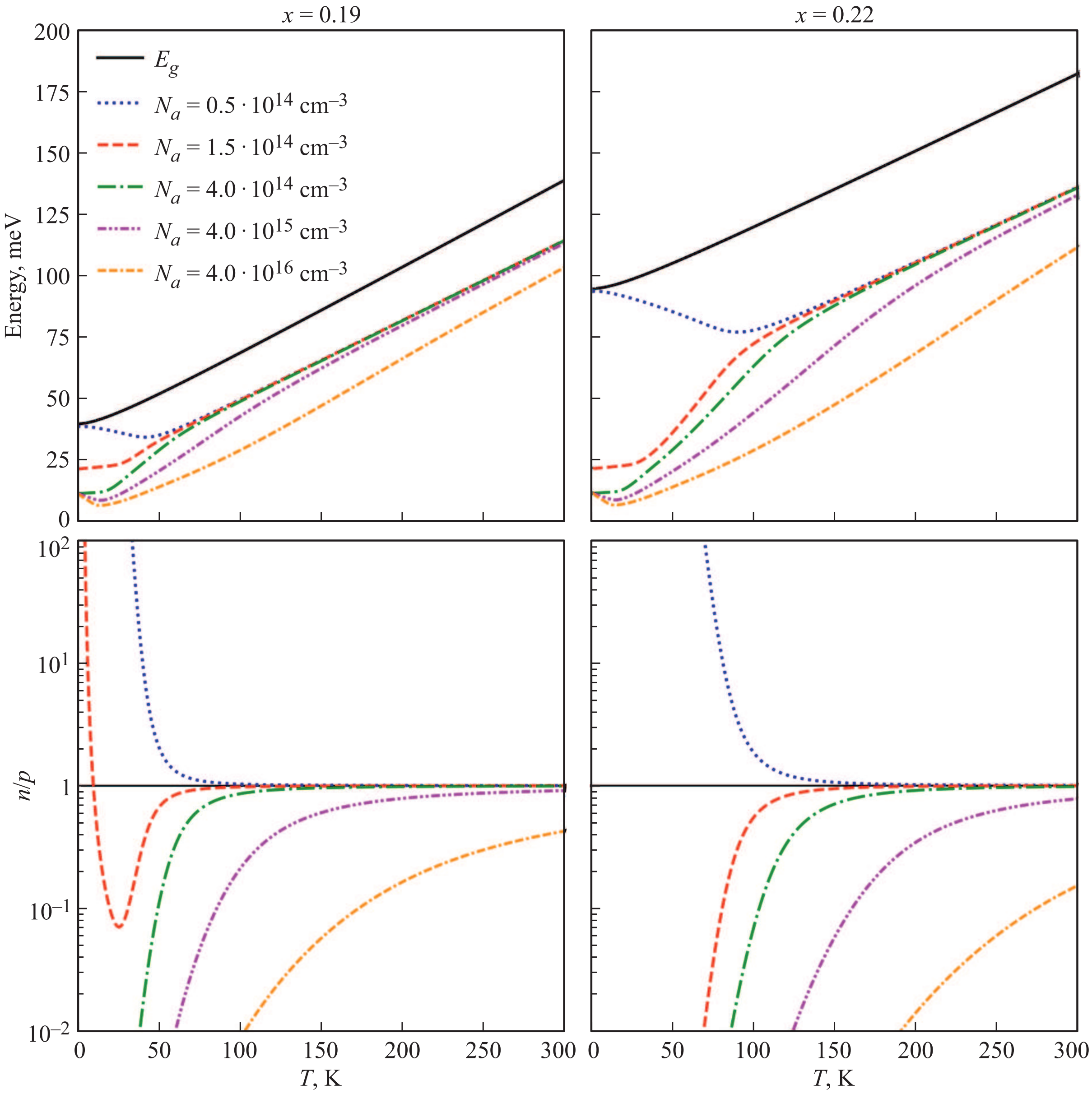

Figure 2. Calculated dependence of the Fermi level position and the relative concentration of electrons and holes on temperature at various degrees of compensation of mercury vacancies by donors. The donor concentration is fixed and equal to $2 \cdot 10^{14}$ cm^{-3}. (Colored version of the figure is presented in electronic version of the article).

$2 \cdot 10^{14}$ cm^{-3}. Dotted line shows the concentration of holes thermally ionized into the continuum from neutral centers. It can be seen that up to 30 K, the concentration of ionized centers coincides with the total number of holes occurring in the valence band. Thus, up to 30 K, neutral A_2^0-centers are sources of free holes. At $T > 40$ K, the concentration of carriers ionized from neutral vacancies approaches to $2 \cdot 10^{14}$ cm^{-3}, i.e., to the concentration of neutral acceptors at low temperatures. Consequently, neutral mercury vacancies at $T > 40$ K are practically absent.

It is also seen in Fig. 1 that, up to 60 K, the concentration of holes ionized from all acceptor centers practically coincides with the number of free carriers in the valence band, i.e., up to 60 K, mercury vacancies are the source of holes in the continuum. As the temperature increases > 60 K, the noticeable contribution of the interband thermal excitation of carriers to the conductivity appears. In this case, the acceptor states are emptied: at low temperature in the CHT structure under consideration with the concentration of mercury vacancies of $4 \cdot 10^{14}$ cm^{-3} and compensating donors of $2 \cdot 10^{14}$ cm^{-3} the concentration of holes bonded at acceptor levels is $6 \cdot 10^{14}$ cm^{-3}. It can be seen from Fig. 1 that at temperature of 70 K the concentration of holes ionized into the valence band from mercury vacancy states is $\sim 5 \cdot 10^{14}$ cm^{-3}, i.e., more than 80% of the acceptor centers lose their carriers.

Thus, it follows from the performed calculations that up to 30 K, holes donate neutral mercury vacancies to the valence band, then, as the temperature rises, A_2^{-1}-centers begin to take part in the formation of conductivity, and for $T > 40$ K such centers become the main source of carriers in the continuum, and as the temperature increases $T > 60$ K, the transition to intrinsic conduction begins.

Figure 2 shows the position of the Fermi level in the band gap for different compositions of the solid-state solution ($x = 19$ and 22%) at different concentrations of mercury vacancies. Solid line shows the position of the conduction band bottom. The band gap at zero temperature is $E_g(T = 0) = 39.4$ meV for $x = 19\%$ and $E_g(T = 0) = 94.3$ meV for $x = 22\%$ [26]. It can be seen that at high temperature, when the conductivity becomes intrinsic, the Fermi level shifts parallel to the edge of the conduction band with the change in temperature. At low concentration of mercury vacancies ($4 \cdot 10^{14}$ cm^{-3}), the energy gap between the Fermi level and the conduction band bottom in the temperature range of 200−300 K is approximately equal to half of the band gap at low temperature ($E_g(T = 0)/2$). This directly follows from the law of mass action in the self-conduction mode $n = p$.

At higher concentration of vacancies, the Fermi level shifts from the conduction band edge to the depth of the band gap. At the same time, due to the significant difference in the mobilities of electrons μ_n and holes μ_p (typical expression $\mu_n/\mu_p \sim 200$ [27]), the section of sharp exponential increase in the dependence of the specific conductivity $\sigma(T)$ with increasing temperature will also appear in this case, however, the adequate slope in the rectifying coordinates will correspond to an energy substantially greater than $E_g(T = 0)/2$, since the condition $n = p$ is not satisfied. This is illustrated in Fig. 3, which shows the characteristic view for the dependence of the logarithm of specific conductivity $\sigma(T)$ on temperature. Figure 3 also shows the logarithm of parameter $\sigma/T^{3/2}$, which makes it possible to eliminate the factor of increasing for carrier concentrations due to an increase in the effective density of states with temperature. On all curves at high temperatures, the segment of fast quasi-exponential growth of $\sigma(T)$ is noticeable. Approximation of this segment by linear function allows one to determine the activation energy. For the concentration of mercury vacancies $4 \cdot 10^{14}$ cm^{-3} this energy is close to half of the band gap at 0 K, and for the concentration of mercury vacancies $4 \cdot 10^{16}$ cm^{-3} this energy increases by more than 2 times. Please note that the temperature factor $T^{3/2}$ makes a significant contribution to the observed activation energy for $\ln \sigma(T)$, therefore, analysis of the curve without normalization for the dependence of the effective density of states on temperature will lead to significant errors.

This should be taken into account when determining the thermal band gap of the sample with previously unknown concentrations of vacancies and compensating donors. For large concentrations of mercury ($4 \cdot 10^{16}$ cm^{-3}), the $n = p$ condition will be satisfied only in the range well above 300 K, in which measurements are difficult due to material degradation. On the other hand, fairly sharp dependence of the Fermi level position on the parameters of „doping“ and compensation makes it possible to determine the degree of compensation and the concentration of vacancies in the HgCdTe layer under study by means of comparing the optical band gap with the observed scale of the exponential increase in conductivity.

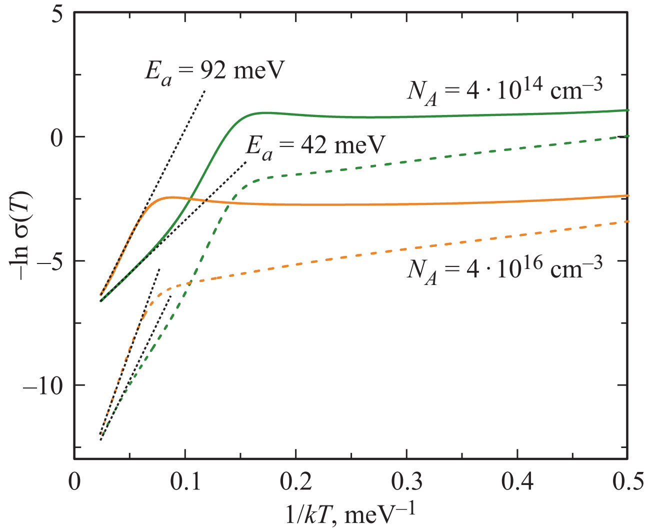

Figure 3. Calculated dependences of the logarithm of the values σ (solid lines) and $\sigma/T^{3/2}$ (dotted lines) on the temperature for the CHT film with 22% of cadmium at different concentrations of mercury vacancies N_A. The donor concentration is fixed and equal to $2 \cdot 10^{14}$ cm^{-3}. It was assumed in the calculation that $\mu_n/\mu_p = 200$.

4. Conclusion

In this paper, the populations of continuum states and mercury vacancy states in narrow-bandgap solid-state solutions of CHT are calculated. It is shown that the temperature quenching of the PC lines associated with an increase in the dark concentration of holes occurs at the temperature of ~ 15 K, which is much lower than the characteristic temperature at which the ratio between the concentrations of neutral and singly ionized vacancies begins to change significantly. Thus, direct observation of the temperature dynamics of the PC lines associated with neutral and singly ionized vacancies is difficult. It is shown that in the range of typical concentrations of mercury vacancies, the transition to intrinsic conductivity in volume films with $x \sim 20\%$ begins at temperatures $T > 60$ K, however, for acceptor concentrations $> 4 \cdot 10^{14}$ cm^{-3} the self-conductivity condition $n = p$ is satisfied with sufficient accuracy only at temperatures > 300 K, which does not allow estimating the band gap based on the law of mass action. The results of rigorous calculations given in this work can be used to determine the concentration of mercury vacancies from the dependence of the conductivity of the electron concentration on temperature.

Funding

The calculation of the Fermi level position and the concentration of carriers in the intrinsic conductivity region was supported by a joint project of the Russian Foundation for Basic Research (RFBR-NNIO_a grant No. 21-52-12020) and German Research Foundation (DFG Project No. 448961446).

The state population calculations for mercury vacancies were supported by the grant from the Ministry of Science and Higher Education (grant of the President of the Russian Federation for state support of young Russian scientists MK-1430.2020.2).

Conflict of interest

The authors declare that they have no conflict of interest.

References

[1] W. Lei, J. Antoszewski, L. Faraone. Appl. Phys. Rev., **2** (4), 041303 (2015).
[2] A. Rogalski. Opto-Electron. Rev., **20** (3), 279 (2012).
[3] A. Rogalski. Rep. Progr. Phys., **68** (10), 2267 (2005).
[4] V.S. Varavin, V.V. Vasiliev, S.A. Dvoretsky, N.N. Mikhailov, V.N. Ovsyuk, Y.G. Sidorov, A.O. Suslyakov, M.V. Yakushev, A.L. Aseev. Proc. SPIE, **5136**, 381 (2003).
[5] S. Dvoretsky, N. Mikhailov, Y. Sidorov, V. Shvets, S. Danilov, B. Wittman, S. Ganichev. J. Electron. Mater., **39** (7), 918 (2010).
[6] N.N. Mikhailov, R.N. Smirnov, S.A. Dvoretsky, Yu.G. Sidorov, V.A. Shvets, E.V. Spesivtsev, S.V. Rykhlitski. Int. J. Nanotechnol., **3** (1), 120 (2006).
[7] B.A. Bernevig, T.L. Hughes, S.C. Zhang. Science, **314** (5806), 1757 (2006).
[8] C. Brüne, C.X. Liu, E.G. Novik, E.M. Hankiewicz, H. Buhmann, Y.L. Chen, X.L. Qi, Z.X. Shen, S.C. Zhang, L.W. Molenkamp. Phys. Rev. Lett., **106** (12), 126803 (2011).
[9] B. Buttner, C.X. Liu, G. Tkachov, E.G. Novik, C. Brune, H. Buhmann, E.M. Hankiewicz, P. Recher, B. Trauzettel, S.C. Zhang, L.W. Molenkamp. Nature Physics, **7** (5), 418 (2011).
[10] F. Teppe, M. Marcinkiewicz, S.S. Krishtopenko, S. Ruffenach, C. Consejo, A.M. Kadykov, W. Desrat, D. But, W. Knap, J. Ludwig, S. Moon, D. Smirnov, M. Orlita, Z. Jiang, S.V. Morozov, V.I. Gavrilenko, N.N. Mikhailov, S.A. Dvoretskii. Nature Commun., **7**, 12576 (2016).
[11] D.B. But, M. Mittendorff, C. Consejo, F. Teppe, N.N. Mikhailov, S.A. Dvoretskii, C. Faugeras, S. Winnerl, M. Helm, W. Knap, M. Potemski, M. Orlita. Nature Photonics, **13** (11), 783-787 (2019).
[12] M. Orlita, D.M. Basko, M.S. Zholudev, F. Teppe, W. Knap, V.I. Gavrilenko, N.N. Mikhailov, S.A. Dvoretskii, P. Neugebauer, C. Faugeras, A.L. Barra, G. Martinez, M. Potemski. Nature Physics, **10** (3), 233 (2014).
[13] G. Alymov, V. Rumyantsev, S. Morozov, V. Gavrilenko, V. Aleshkin, D. Svintsov. ACS Photonics, **7** (1), 98 (2020).
[14] S.V. Morozov, V.V. Rumyantsev, M.S. Zholudev, A.A. Dubinov, V.Y. Aleshkin, V.V. Utochkin, M.A. Fadeev, K.E. Kudryavtsev, N.N. Mikhailov, S.A. Dvoretskii, V.I. Gavrilenko, F. Teppe. ACS Photonics, **8** (12), 3526 (2021).
[15] S. Krishnamurthy, M.A. Berding, Z.G. Yu. J. Electron. Mater., **35** (6), 1369 (2006).
[16] J. Shao, X. Lü, S. Guo, W. Lu, L. Chen, Y. Wei, J. Yang, L. He, J. Chu. Phys. Rev. B, **80** (15), 5125 (2009).
[17] X. Zhang, J. Shao, L. Chen, X. Lü, S. Guo, L. He, J. Chu. J. Appl. Phys., **110** (4), 043503 (2011).
[18] F. Gemain, I.C. Robin, G. Feuillet. J. Appl. Phys., **114** (21), 213706 (2013).
[19] K.D. Mynbaev, A.V. Shilyaev, N.L. Bazhenov, A.I. Izhnin, I.I. Izhnin, N.N. Mikhailov, V.S. Varavin, S.A. Dvoretsky. Semiconductors, **49** (3), 367 (2015).
[20] M.V. Yakushev, K.D. Mynbaev, N.L. Bazhenov, V.S. Varavin, N.N. Mikhailov, D.V. Marin, S.A. Dvoretsky, Y.G. Sidorov. Phys. Status Solidi C, **13** (7–9), 469 (2016).
[21] S.G. Pavlov, L.M. Portsel, V.B. Shuman, A.N. Lodygin, Y.A. Astrov, N.V. Abrosimov, S.A. Lynch, V.V. Tsyplenkov, H.W. Hübers. Phys. Rev. Mater., **5** (11), 114607 (2021).
[22] D.V. Kozlov, V.V. Rumyantsev, S.V. Morozov, A.M. Kadykov, M.A. Fadeev, M.S. Zholudev, V.S. Varavin, N.N. Mikhailov, S.A. Dvoretsky, V.I. Gavrilenko, F. Teppe. ZhETF ,**154**, 1226 (2018)
[23] D.V. Kozlov, T.A. Uaman Svetikova, A.V. Ikonnikov, V.V. Rumyantsev, A.A. Razova, M.S. Zholudev, N.N. Mikhailov, S.A. Dvoretsky, V.I. Gavrilenko, S.V. Morozov. Pis'ma ZhETF, **113** (6), 399 (2021) (in Russian).
[24] V.V. Rumyantsev, D.V. Kozlov, S.V. Morozov, M.A. Fadeev, A.M. Kadykov, F. Teppe, V.S. Varavin, M.V. Yakushev, N.N. Mikhailov, S.A. Dvoretskii, V.I. Gavrilenko. Semicond. Sci. Techn., **32** (9), 095007 (2017).
[25] P.A. Bakhtin, S.A. Dvoretsky, V.S. Varavin, A.P. Korobkin, N.N. Mikhailov, I.V. Sabinina, Yu.G. Sidorov. FTP, **38** (10), 1207 (2004) (in Russian).
[26] J.P. Laurenti, J. Camassel, A. Bouhemadou, B. Toulouse, R. Legros, A. Lusson. J. Appl. Phys., **67** (10), 6454 (1990).
[27] P.S. Wijewarnasuriya, M. Boukerche, J.P. Faurie. J. Appl. Phys., **67** (2), 859 (1990).